AFCRL-72-0455

LASER INDUCED DAMAGE TO NONLINEAR OPTICAL MATERIALS

BY

C.R. GIULIANO AND D.Y. TSENG

HUGHES RESEARCH LABORATORIES
A DIVISION OF HUGHES AIRCRAFT COMPANY
3011 MALIBU CANYON ROAD MALIBU,
CALIFORNIA 90265

CONTRACT NO. F33615-71-C-1715
PROJECT NO. 6100
TASK NO. 610001
WORK UNIT NO. 61000101

FINAL REPORT
1 JUNE - 1971 - 1 JUNE 1972
SEPTEMBER 1972

CONTRACT MONITOR: DAVID MILAM
OPTICAL PHYSICS LABORATORY

PREPARED FOR

AIR FORCE CAMBRIDGE RESEARCH LABORATORIES
AIR FORCE SYSTEMS COMMAND
UNITED STATES AIR FORCE
BEDFORD, MASSACHUSETTS 01730

DOCUMENT CONTROL DATA - R&D

(Security classification of title, body of abstract and indexing annotation must be entered when the overall report is classified)

1. ORIGINATING ACTIVITY *(Corporate author)*
Hughes Research Laboratories
3011 Malibu Canyon Road,
Malibu, California 90265

2a. REPORT SECURITY CLASSIFICATION
Unclassified

2b. GROUP

3. REPORT TITLE

LASER INDUCED DAMAGE TO NONLINEAR OPTICAL MATERIALS

4. DESCRIPTIVE NOTES *(Type of report and inclusive dates)*
Scientific. Final. 1 June 1971 - 1 June 1972 Approved 17 Aug. 1972

5. AUTHOR(S) *(First name, middle initial, last name)*
C.R. Giuliano
D.Y. Tseng

6. REPORT DATE	7a. TOTAL NO. OF PAGES	7b. NO. OF REFS
September 1972	39	7

8a. CONTRACT OR GRANT NO.	9a. ORIGINATOR'S REPORT NUMBER(S)
F33615-71-C-1715	
b. PROJECT, TASK, WORK UNIT NOS. C100-01-01	
c. DOD ELEMENT 62204F	9b. OTHER REPORT NO(S) *(Any other numbers that may be assigned this report)* AFCRL-72-0455
d. DOD SUBELEMENT 616100	

10. DISTRIBUTION S

DISTRIBUTION STATEMENT A
Approved for public release;
Distribution Unlimited

Details of illustrations in this document may be better studied on microfiche

11. SUPPLEMENTARY NOTES	12. SPONSORING MILITARY ACTIVITY
TECH, Other	Air Force Cambridge Research Laboratories (OP) L.G. Hanscom Field Bedford, MA 01730

13. ABSTRACT

This report incorporates the results of an experimental study of laser induced damage in lithium iodate ($LiIO_3$) and proustite (Ag_3AsS_3) at 1.06 and 0.694 μm using lasers with well-characterized output properties. The main objective of the $LiIO_3$ investigation was to determine if a significant difference in damage threshold between phase matched (PM) and non-PM conditions for second-harmonic generation (SHG) exists. The objective of the proustite work was to measure surface damage threshold as a function of pulse repetition rate. No significant difference was found in bulk damage thresholds for $LiIO_3$ between PM and non-PM under the following experimental conditions: single pulse operation at 0.694 and 1.06 μm and 10 pps at 1.06 μm for 20% SHG. Damage threshold power densities were about 2 GW/cm^2 for 20 nsec pulses. For proustite it was found that entrance surface damage threshold occurred at a constant pulse peak power density (or energy density) independent of pulse repetition rate over the range from single shot to 500 pps at 1.06 μm. Damage thresholds at 1.06 μm were about 0.4 J/cm^2 for a 240 nsec pulse (1.6 MW/cm^2) and at 0.694 μm J/cm^2 for a 20 nsec pulse (60 MW/cm^2).

DD FORM 1 NOV 63 1473

14. KEY WORDS	LINK A		LINK B		LINK C	
	ROLE	WT	ROLE	WT	ROLE	WT
Lithium Iodate						
Proustite						
Phase Matching						
Laser Damage						
0.694 and 1.06 μm						
Single and Multiple Pulse Operation						

A2

AFCRL-72-0455

LASER INDUCED DAMAGE TO NONLINEAR OPTICAL MATERIALS

by

C.R. Giuliano and D.Y. Tseng

Hughes Research Laboratories
A Division of Hughes Aircraft Company
3011 Malibu Canyon Road
Malibu, California 90265

Contract No. F33615-71-C-1715
Project No. 6100
Task No. 610001
Work Unit No. 61000101

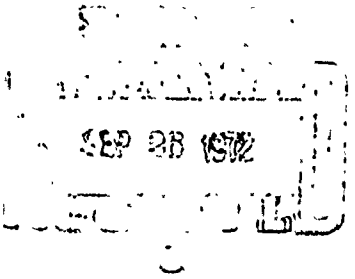

FINAL REPORT

1 June 1971 – 1 June 1972

September 1972

Contract Monitor: David Milam
Optical Physics Laboratory

This document is subject to special export controls and each transmittal to foreign governments or foreign nationals may be made only with prior approval of AFAL (TEL).

Prepared for

AIR FORCE CAMBRIDGE RESEARCH LABORATORIES
AIR FORCE SYSTEMS COMMAND
UNITED STATES AIR FORCE
BEDFORD, MASSACHUSETTS 01730

ABSTRACT

This report incorporates the results of an experimental study of laser induced damage in lithium iodate ($LiIO_3$) and proustite (Ag_3AsS_3) at 1.06 and 0.694 μm using lasers with well-characterized output properties. The main objective of the $LiIO_3$ investigation was to determine if a significant difference in damage threshold between phase matched (PM) and non-PM conditions for second-harmonic generation (SHG) exists. The objective of the proustite work was to measure surface damage threshold as a function of pulse repetition rate. No significant difference was found in bulk damage thresholds for $LiIO_3$ between PM and non-PM under the following experimental conditions: single pulse operation at 0.694 and 1.06 μm and 10 pps at 1.06 μm for 20% SHG. Damage threshold power densities were about 2 GW/cm^2 for 20 nsec pulses. For proustite it was found that entrance surface damage threshold occurred at a constant pulse peak power density (or energy density) independent of pulse repetition rate over the range from single shot to 500 pps at 1.06 μm. Damage thresholds at 1.06 μm were about 0.4 J/cm^2 for a 240 nsec pulse (1.6 MW/cm^2) and at 0.694 μm, 1 J/cm^2 for a 20 nsec pulse (60 MW/cm^2).

FOREWORD

This is the Final Technical Report on Contract F33615-71-C-1715. The work reported herein was accomplished at Hughes Research Laboratories, 3011 Malibu Canyon Road, Malibu, California. This publication documents research done during the period 1 June 1971 to 1 June 1972.

This report was submitted by the authors July 1972. The Air Force Contract Monitor was David Milam.

Principal investigators were C. R. Giuliano and D. Y. Tseng. P. O. Clark, Laser Department Manager, and V. Evtuhov, Quantum Electronics Section Head, served in an advisory capacity.

TABLE OF CONTENTS

LIST OF ILLUSTRATIONS

SECTION I

INTRODUCTION

This report contains the summation of the results of a one-year study of laser induced damage in nonlinear optical materials. Within the bounds of this program, the work was concentrated on the comparison of two different materials, lithium iodate ($LiIO_3$) and proustite (Ag_3AsS_3) studied at both 1.06 and 0.694 μm, with the main emphasis at 1.06 μm. For this purpose, mode controlled lasers with well-characterized smooth spatial profiles were used. The main purpose of the work on $LiIO_3$ was to find out whether a significant difference exists between damage thresholds for phase matched (PM) compared with non-PM conditions for second harmonic generation. For these experiments, bulk damage was studied instead of surface damage because in most second-harmonic generators, the light at the fundamental is focused inside the nonlinear crystal and internal damage usually occurs first. For proustite, the main goal was to determine the dependence of damage threshold on peak power and repetition rate in the hope of determining the character of the damage mechanism.

The details of the experiments and the procedure used for characterizing the laser beam profiles are contained in Section II, Technical Discussion, of this report which is divided into four main sections. In Section II-A and II-B we discuss the details of our experiments on $LiIO_3$ and proustite, respectively. Some discussion of damage morphology is given, and the results are tabulated and reviewed. Section II-C describes the lasers used for this program, and Section II-D contains a description of the approach and methods used for measuring beam profiles and spot sizes for the lasers of interest.

The results for $LiIO_3$ indicate that there is no appreciable difference between damage thresholds for PM and non-PM conditions. The experimental conditions under which this conclusion is valid are 20 to 25% second-harmonic conversion at 1.06 μm for both single pulse

and 10 pps operation and for single pulse operation at 0.694 μm. The results for proustite show that the damage threshold peak power density for one of the types of surface damage is independent of repetition rate from single pulse operation to 500 pps. (Refer to Section II-B-1 for a detailed description of the different types of surface damage.)

SECTION II

TECHNICAL DISCUSSION

A. LITHIUM IODATE ($LiIO_3$) DAMAGE STUDIES

The main purpose of our damage experiments in $LiIO_3$ has been to explore whether damage occurs more easily under phase matched (PM) conditions than for non-PM conditions. Various workers[1,2] have reported that this occurs for certain materials used as frequency doublers, but in many of these experiments the observations were not well defined under controlled conditions. In our experiments we chose to look at $LiIO_3$ both phase matched and non-phase matched for second-harmonic generation at 1.06 μm and 6943 Å. At these two wavelengths the doubling was accomplished external to the cavity, and the experiments were carried out under both single pulse and repetitively pulsed conditions. For all the experiments performed we observed no significant difference in the thresholds between PM and non-PM conditions. Details of the experiments and the conditions under which damage was studied are outlined in the following subsections.

1. Damage Morphology in $LiIO_3$

The internal damage formed close to threshold in $LiIO_3$ consists of one or two small cracks about 20 μm across. If the damage is formed well above threshold or if one of the small threshold sites is exposed repeatedly to additional pulses (as often happens in the 10 pps experiments), the damaged area is appreciably larger, and the center of the fractured region is brownish in color suggesting the presence of free iodine. In fact it is possible to smell iodine when a sample has been very extensively damaged (usually accidentally). The internal damage sites vary somewhat in their location inside the crystal. The extent of this variation in damage location depends on the particular sample and appears to be a function of the density of internal scattering sites or

small inclusions. In some of the better quality samples, the damage was most often found close to the focal region.

If a damaged region is repeatedly exposed to additional damaging pulses, the damaged region grows in an upstream direction giving the appearance of a track. This track, however, grows relatively slowly (approximately one second at 10 pps) and although reminiscent of a self-focusing track does not arise from self-focusing. It is merely the result of a continued deposition of energy at the upstream end of a damaged region. Self-focusing damage has been observed occasionally when samples were subjected to single shots well above threshold.

2. $LiIO_3$ Damage at 6943Å

Two ruby lasers were used to obtain damage thresholds in $LiIO_3$ at 6943 Å. They are described in Section II-C. The single pulse Q-switched ruby laser was employed early in the program and only one sample was studied extensively. It was found that for single pulse operation there was no difference between damage thresholds measured for PM and non-PM conditions. (Threshold values are listed in Table I.) The continuously pumped, repetitively Q-switched ruby laser was also employed in the early stages of the program when $LiIO_3$ damage was first being explored. No detailed quantitative data were obtained using this laser because several difficulties arose which made it extremely difficult to operate reliably. The main problem was the reliability factor of the high pressure mercury arc lamps used in the pump cavity. The particular lamp used in the early stages of the program failed after many hours of reliable operation. Subsequent lamps proved to be much shorter lived; hence experiments were constantly interrupted. Other problems with balancing the rotating mirror Q-switch led to fluctuations in the peak power from shot to shot, making it impossible to obtain reliable quantitative data at that time. Meanwhile, the high power Nd:YAG laser (10 pps) became available and we concentrated on using it for the rest of the program.

Although no quantitative data were obtained with the repetitively Q-switched ruby laser, we were able to gain experience in the identification of damage morphology in $LiIO_3$ and to become familiar with the various problems in handling and examining these materials.

3. $LiIO_3$ Damage at 1.06 μm

For these measurements the high power pulsed Nd:YAG laser described in Section II-C-1 was used. (A few attempts were made to obtain damage with the low power Nd:YAG laser, but we were unable to reach damage threshold.) The experimental setup used is shown in Fig. 1. The light is focused inside the samples (typically 1 cm cubes) using a 3.5 cm focal length lens. Incident power is monitored using a silicon photodiode and in the phase matching experiments, the second harmonic is also monitored with a photomultiplier tube placed beyond the sample. In the single pulse experiments, the power was monitored for each shot; in the experiments carried out at 10 pps, several shots (~10) were superimposed and photographed on the oscilloscope screen. To change from PM to non-PM conditions the sample was rotated slightly (~0.5°), such that the second-harmonic intensity was seen to drop about two orders of magnitude from the optimum. In this way, damage thresholds were measured for both conditions in the same sample.

A typical set of experiments would consist of the following procedure. The sample would be irradiated at a level generally below threshold and examined between irradiations for the presence of damage. If no damage was seen to have occurred, the incident power level would be increased (10 to 20%) and the sample again subjected to another exposure. Examination for internal damage was done by looking visually for light from the He-Ne alignment laser scattered from the damage sites and by viewing the sample through a traveling microscope. For single pulse experiments, the sample was examined after each shot. For 10 pps experiments, a typical exposure would consist of

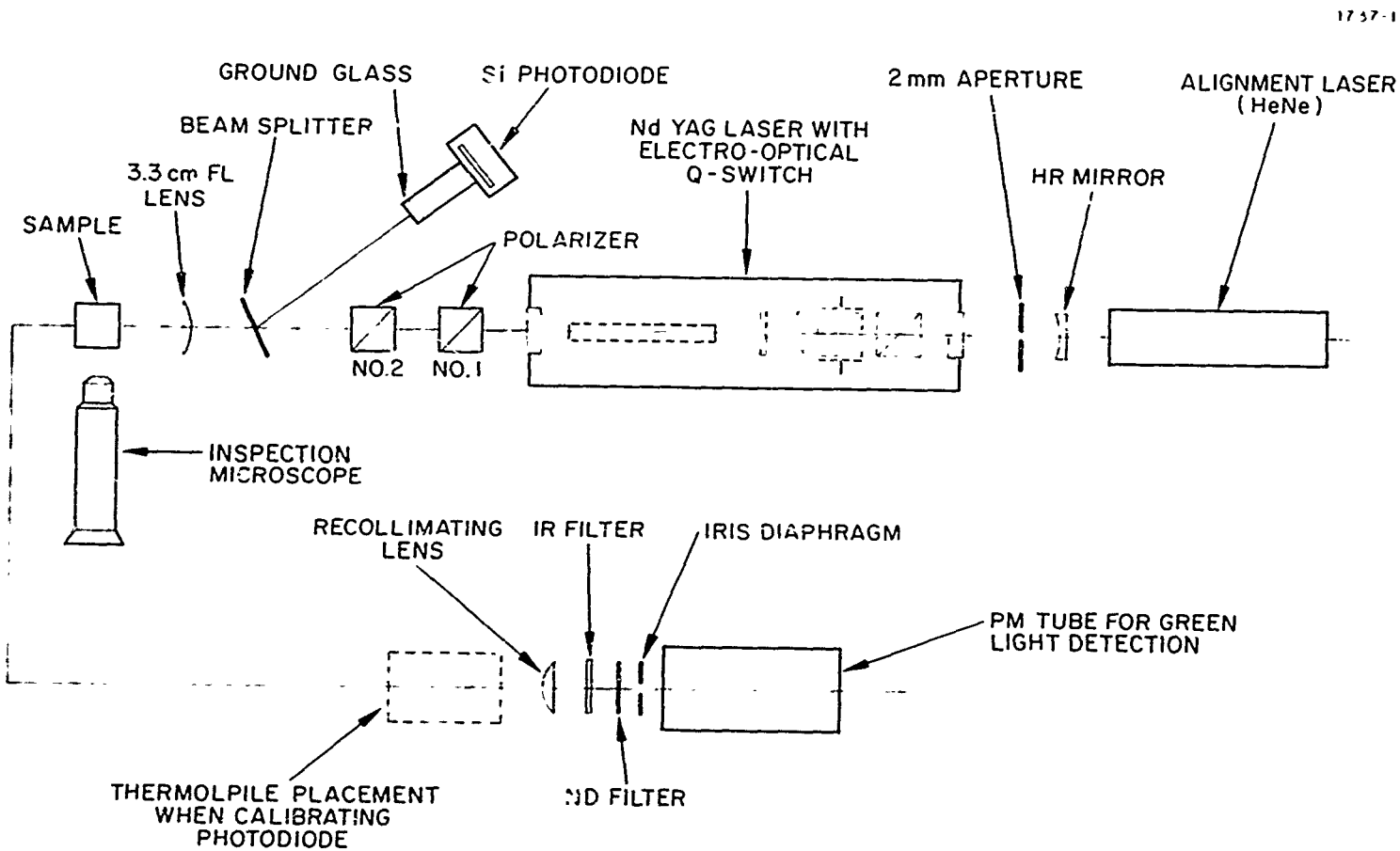

Fig. 1. Experimental setup for damage experiments using high power Nd:YAG laser.

about 30 sec (300 shots) and the sample subsequently examined. In virtually all cases at 10 pps, it is possible to see easily with the unaided eye the incandescence of the internal sites at the time they are formed. In such cases, the beam was quickly interrupted and the exposure time noted. By the time the self-incandescence is noted and the beam interrupted, it is found that the damage is fairly extensive, i.e., the brownish color of iodine in the center of the internal fracture is apparent, indicating that the damage site has been hit more than once after it was formed.

Many experiments were carried out at 10 pps for two different samples under both PM and non-PM conditions. The peak power at which damage was seen to occur from one site to another was fairly variable (see Fig. 2), but for a given damage site the threshold is well defined. To emphasize this point, the following findings summarize our documentation of 50 damage sites on two different crystals.

- In every case, the site in question was subjected to at least 300 shots whose peak powers were between 85 and 90% of the level at which damage finally was seen to occur.
- In 16 cases, the damage site in question was subjected to up to 1200 shots (in one case, 1800 shots) whose peak powers ranged from 65 to 90% of the power at which damage finally occurred.
- When damage level was reached, damage was seen to occur (by observation of incandescence) within 3 sec (30 shots) of exposure to the pulse train.

These results indicate that a given site has well-defined threshold power; whereas the threshold can vary considerably from site to site within the material.

4. Results of $LiIO_3$ Damage Experiments

The results of measurements of bulk damage thresholds in $LiIO_3$ are tabulated in Table I. Samples were obtained from various sources. Many of the samples studied in the early stages were grown

TABLE I

Damage Thresholds for Various Samples of $LiIO_3$

Sample	Wavelength, μm	Pulse Repitition Rate	Damage Threshold Power Density[a], GW/cm^2			Damage Threshold[a] Energy, Density, J/cm^2	Second-Harmonic Conversion, %	No. of Thresholds Measured
			Av Value	Av Deviation	Range	Av Value		
A	1.06	10 pps	1.92	0.23	1.39 to 2.36	35.5	19 to 28	21
A	1.06	10 pps	2.14	0.20	1.80 to 2.77	39.6	0	13
A	1.06	Single Shot	2.01	0.47	1.54 to 2.80	37.2	0	10
A	0.694	Single Shot	2.63	0.52	1.9 to 3.6	52.7	0	12
B	1.06	10 pps	2.16	0.25	1.68 to 2.80	40.0	0	16
B	1.06	Single Shot	1.50	0.40	0.95 to 2.90	27.8	0	11
C	1.06	Single Shot	1.30	0.18	0.98 to 1.85	24.0	0	12
D	1.06	Single Shot	1.34	0.28	1.0 to 2.5	24.8	20	24
D	1.06	Single Shot	1.83	0.28	1.32 to 2.40	34.0	0	10
E	0.694	Single Shot	0.55	0.07	0.36 to 0.70	11.0	0	7
E	0.694	Single Shot	0.60	0.08	0.40 to 0.85	12.0	~10	8

[a]These values are given as total power (or energy) divided by the beam area defined as πa^2, where a is the 1/e radius for the electric field. The on-axis intensities (energy densities) are twice as large as the values quoted in the table.

T604

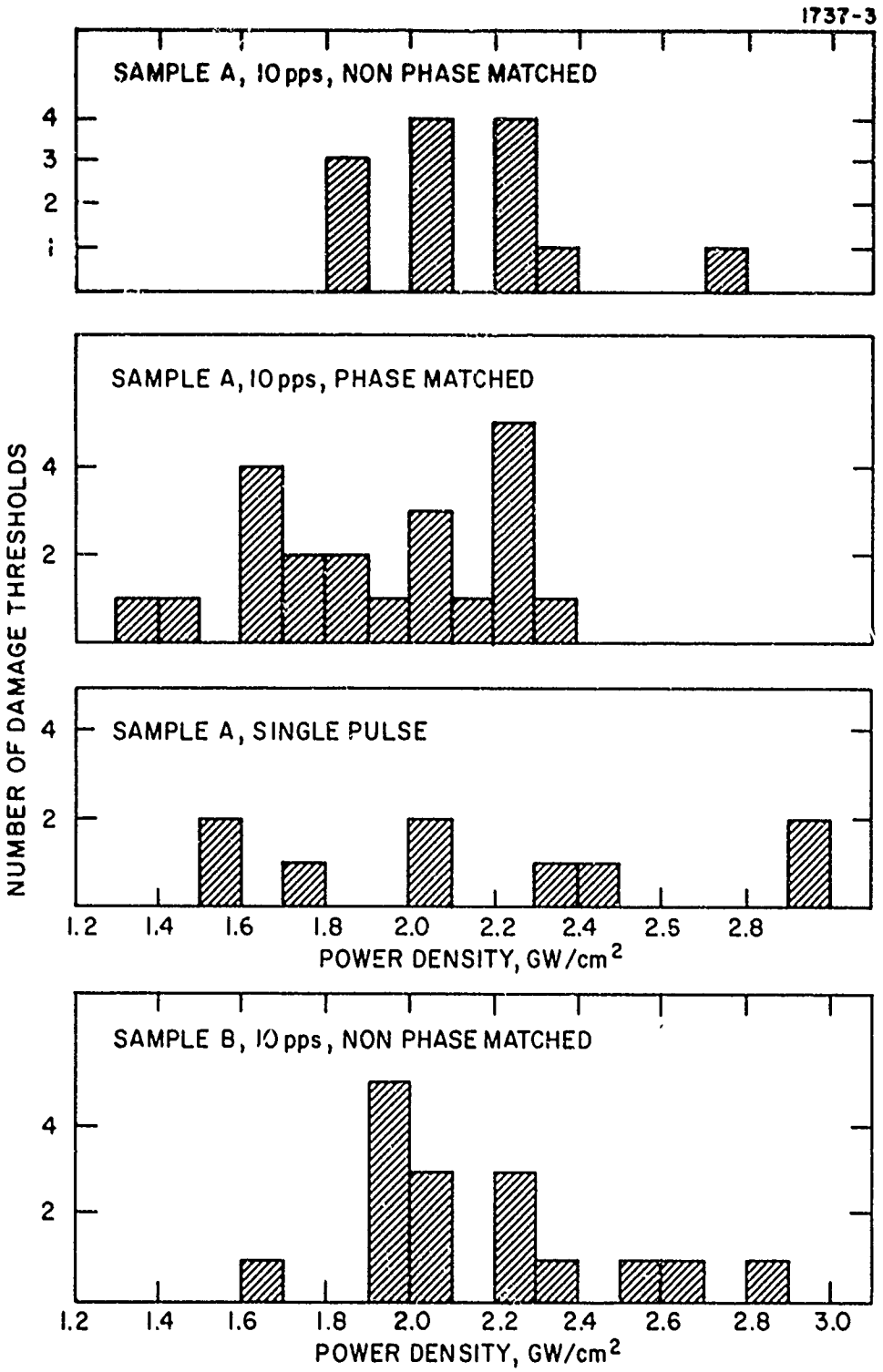

Fig. 2. Number of damage thresholds versus power density for $LiIO_3$ showing distribution of values.

at HRL. Others were obtained from Stanford University,* Isomet, Clevite, and Gsänger. The quality of the material from the different sources did not vary widely; most of the damage threshold values are of about the same order.

The damage threshold measurements at 6943Å were taken early in the program on an HRL grown sample (sample E), the optical quality of which was not as high as samples studied later at 1.06 μm. The low threshold for sample E compared with sample A at 6943Å is probably a reflection of the difference in crystal quality.

A comparison of single shot and 10 pps thresholds for sample B in Table I suggests an appreciable difference between the two. However, it should be noted that the single shot data were taken at an earlier time in the program than the 10 pps data, and a different calibration pertained to that situation. The same is true for the lower thresholds listed for samples C and D (phase matched). Hence, the apparent difference between the group of thresholds around 2 GW/cm^2 and those around 1.4 GW/cm^2 may be a reflection of the reliability of different calibration procedures, although the precision of a given calibration procedure is greater than the above difference.

B. PROUSTITE (Ag_3AsS_3) DAMAGE STUDIES

All the experiments in proustite were entrance surface damage experiments. For these studies the bulk of the measurements were carried out at 1.06 μm using the low power Nd:YAG laser described in Section II-C-2. This laser was operated in the single shot mode, repetitively Q-switched at a repetition rate up to 500 pps, and continuously. A few threshold measurements were also carried out at 6943Å using the single shot ruby laser.

The primary goal of the proustite damage studies was to determine the threshold as a function of pulse repetition rate. This was done at 1.06 μm, and it was found that the damage threshold peak power

*We are grateful to Dr. Robert Byer of the Materials Research Laboratories of Stanford University for providing a sample of $LiIO_3$.

for entrance surface damage (of the type described later as "micromelting") is essentially independent of the pulse repetition rate from single shot operation to 500 pps.

1. Damage Morphology in Proustite

Three distinctly different types of damage are seen on proustite entrance surfaces. The occurrence of a particular type depends on the character of the irradiation (i.e., whether pulsed or continuous) and also to some extent on the quality of the surface finish. The three types are described in the following.

a. Molten Craters

These have been seen to occur only during cw illumination at relatively high cw powers or when a previously created pulse damage site (see below) is illuminated with a relatively low cw power. The formation of these craters is accompanied by a plume of yellow smoke (presumably sulfur), which sometimes settles on the undamaged surface in the vicinity of the crater depending on the direction of air currents in the laboratory. The craters have slightly raised rims and very flat shiny bottoms that appear black in color and are apparently the results of molten puddles of decomposed material. Crater depth is typically 25 μm. This type of damage is the most catastrophic of the three types observed. Examples of this type of damage are seen in Fig. 3.

b. Micromelting

This type of damage occurs with either single pulsed or repetitively pulsed illumination. It is characterized by a series of somewhat randomly spaced tiny molten regions. The number and density of these regions depends both on the local surface finish and the incident power. When the power is appreciably above threshold, the molten regions merge to form a large variegated damage spot. At lower powers there is a tendency for these small globular sites to

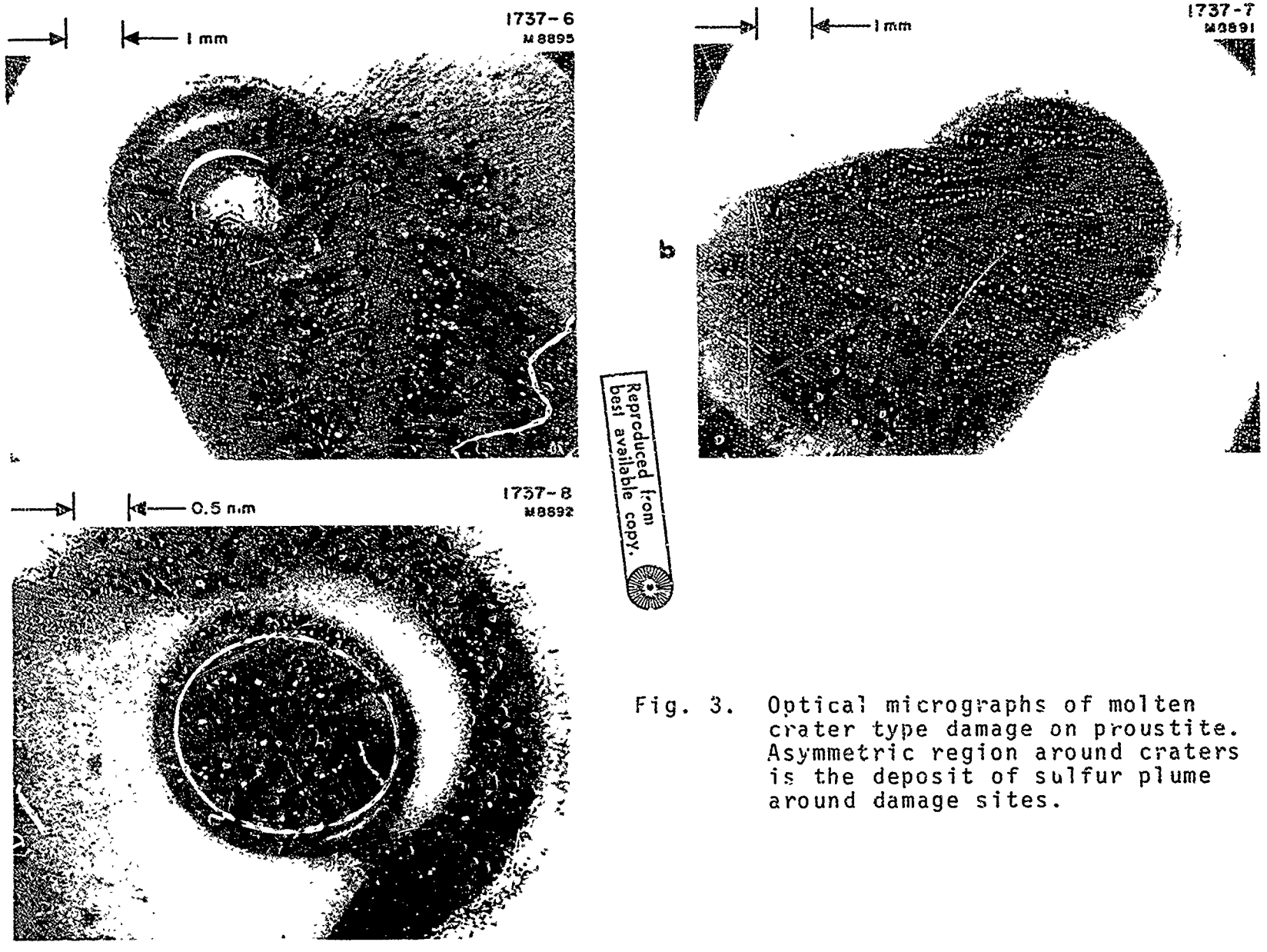

Fig. 3. Optical micrographs of molten crater type damage on proustite. Asymmetric region around craters is the deposit of sulfur plume around damage sites.

cluster along lines of surface scratches. When observed through the low power microscope in the laboratory damage threshold setup, they appear to have a metallic luster and the region in which they are clustered has a darker color than the surrounding undamaged surface. Examples of this type of damage are seen in Figs. 4 and 5.

c. Ghost Sites

This type of damage occurs with continuous illumination at 1.06 μm and was a source of much confusion when first observed. Under low magnification in the laboratory setup, it is similar in appearance to the damage described in (b) above; that is, it appears as a speckled area with a metallic luster. This kind of damage is easily visible with the unaided eye as a small scattering region on the surface. Depending on the incident laser power and exposure time, however, the damage fades within 30 sec to 30 min after the laser is turned off and sometimes disappears completely. This type of damage happens at very low cw power and as the power is increased, takes longer to fade away until finally a power level is reached at which some of the damage appears to be permanent. Ghosting has been seen also at high repetition rate illumination, but only if the surface finish has the cloudy appearance referred to in the previous section.

2. Growth of Proustite Damage under Microscope Illumination

It has been observed that when a laser damaged region on proustite is examined microscopically, under certain conditions growth of the damage continues. This phenomenon was first encountered during the process of obtaining photomicrographs of the different kinds of proustite surface damage. The samples were irradiated with the laser at different levels of intensity and then placed under the objective of a microscope equipped for bright field, reflected light observation. Under these conditions of relatively intense white light illumination, several of the regions immediately surrounding the more extensively damaged sites began to develop additional damage. The new sites

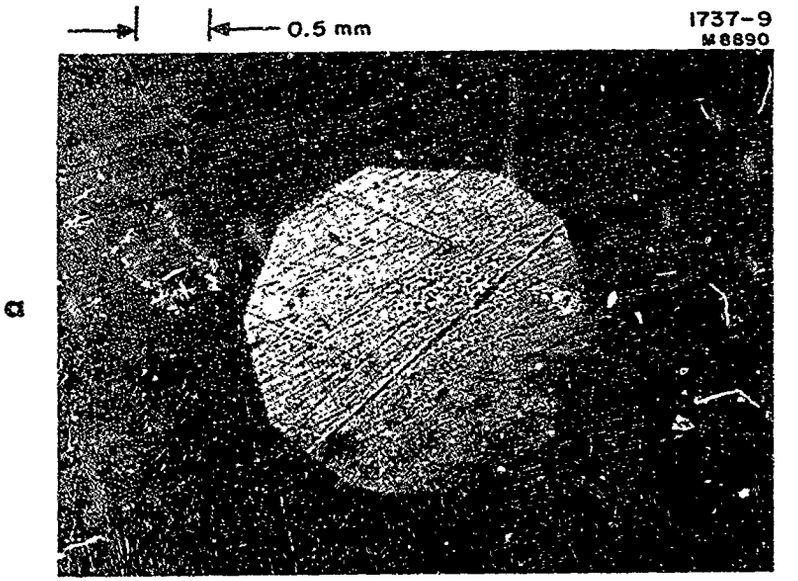

a

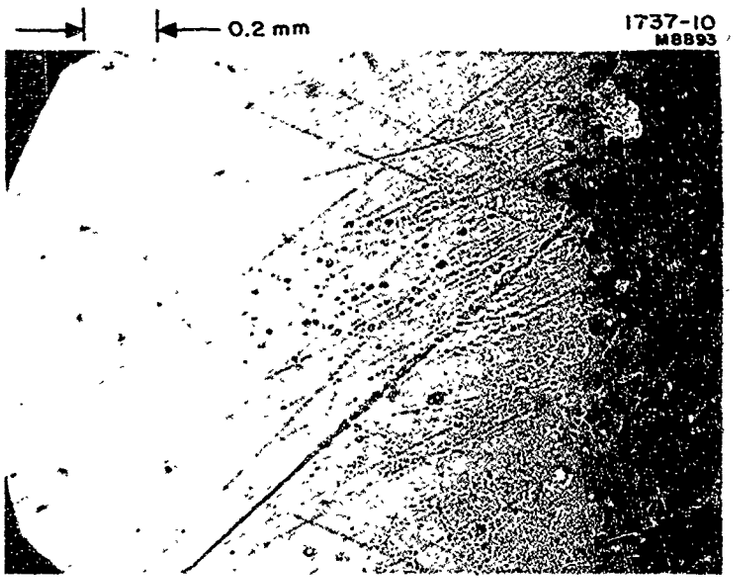

b

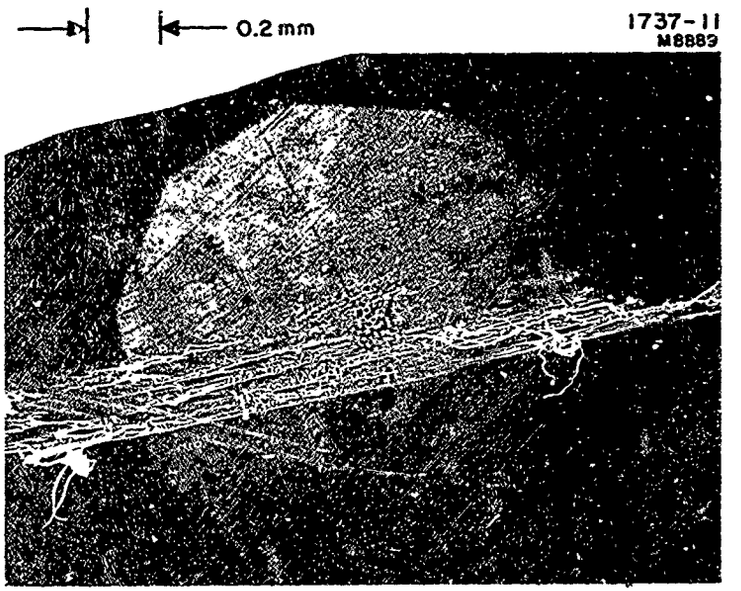

c

Fig. 4. Optical micrographs of micro-melting type damage on proustite surface near damage threshold for pulsed operation. Note clustering of sites around surface scratches.

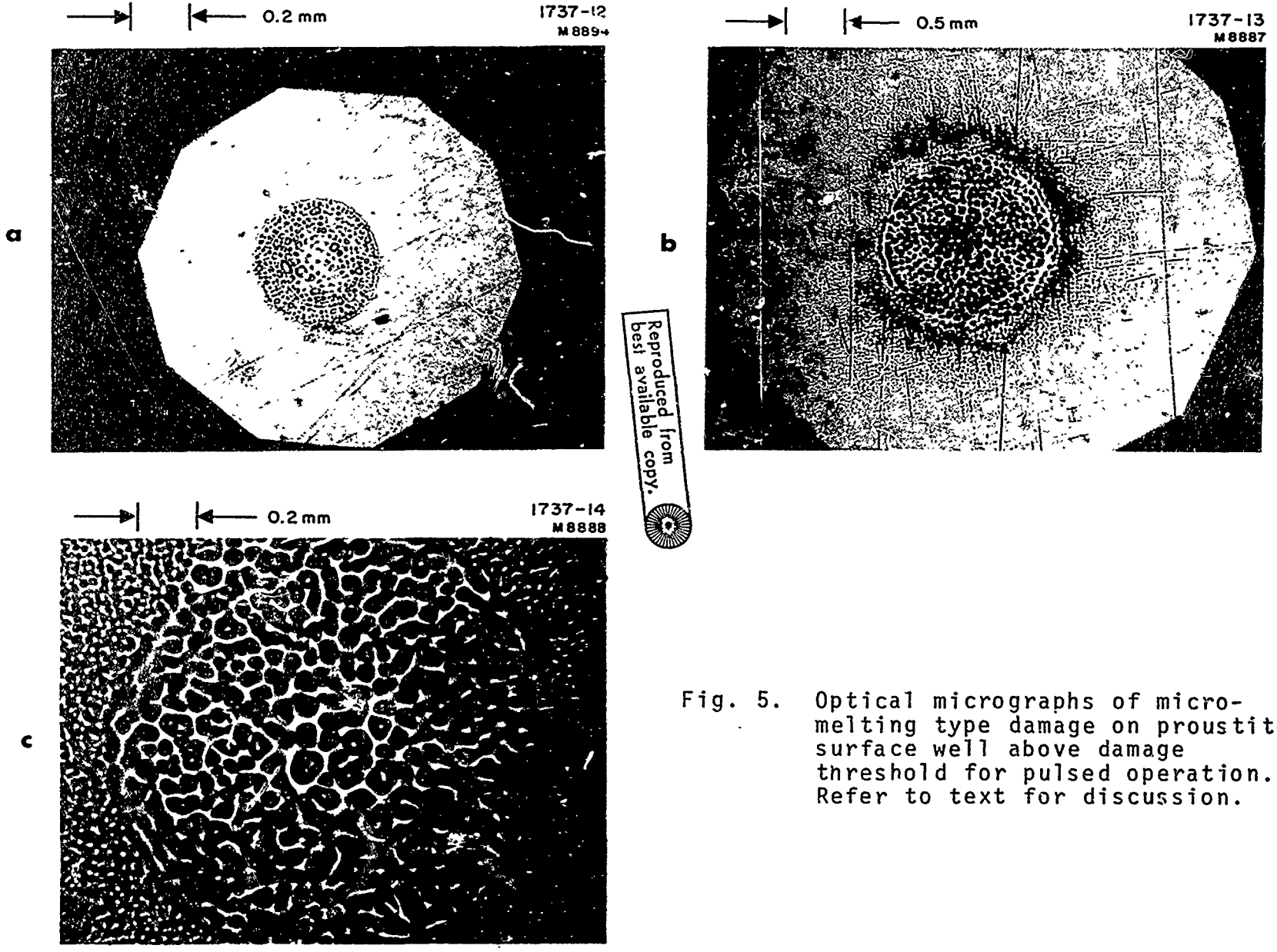

Fig. 5. Optical micrographs of micro-melting type damage on proustite surface well above damage threshold for pulsed operation. Refer to text for discussion.

became visible in about a minute and when left under the microscope light, more sites appeared with time. An example of this is seen in Fig. 5(b) and (c). The region outside of the well-defined circular boundary contains a number of scattered sites that appeared after the sample had been subjected to microscope illumination for some time (~30 min). These should be contrasted with Fig. 5(a), which shows a relatively clear area outside of the circular laser-damaged region. This phenomenon, which was not investigated in detail, is another example of the peculiar nature of proustite damage. It only is seen to occur on previously damaged regions and may be the result of some ejection of decomposed matter from the initial damage sites. With the present limited knowledge of this proustite behavior, its origin can only be conjectured.

3. Experimental Procedure for Damage Measurements in Proustite

The experimental setup for proustite damage threshold measurements is shown in Fig. 6. For single pulse experiments, the laser was fired at a given level initially chosen to be below damage threshold and the sample was examined between shots using a low power (20x) microscope that could be moved in and out without disturbing the sample. If no damage was observed after several shots at a particular level, the power was increased by 5 to 10% and the sample again irradiated until damage was observed. In the repetitively pulsed experiments, a similar method was employed but instead the sample would be exposed for a predetermined time (usually 10 sec) at a given power and subsequently examined for damage. Again, if no damage was seen, the power was increased by 5 to 10% and another exposure made. This procedure was repeated until damage was observed.

The visual detection of damage near inception requires experience and practice in viewing through the microscope and also in choosing the proper illumination of the surface. It was found that many of the more subtle damage areas escaped detection in the earlier stages of this work because of these critical illumination requirements.

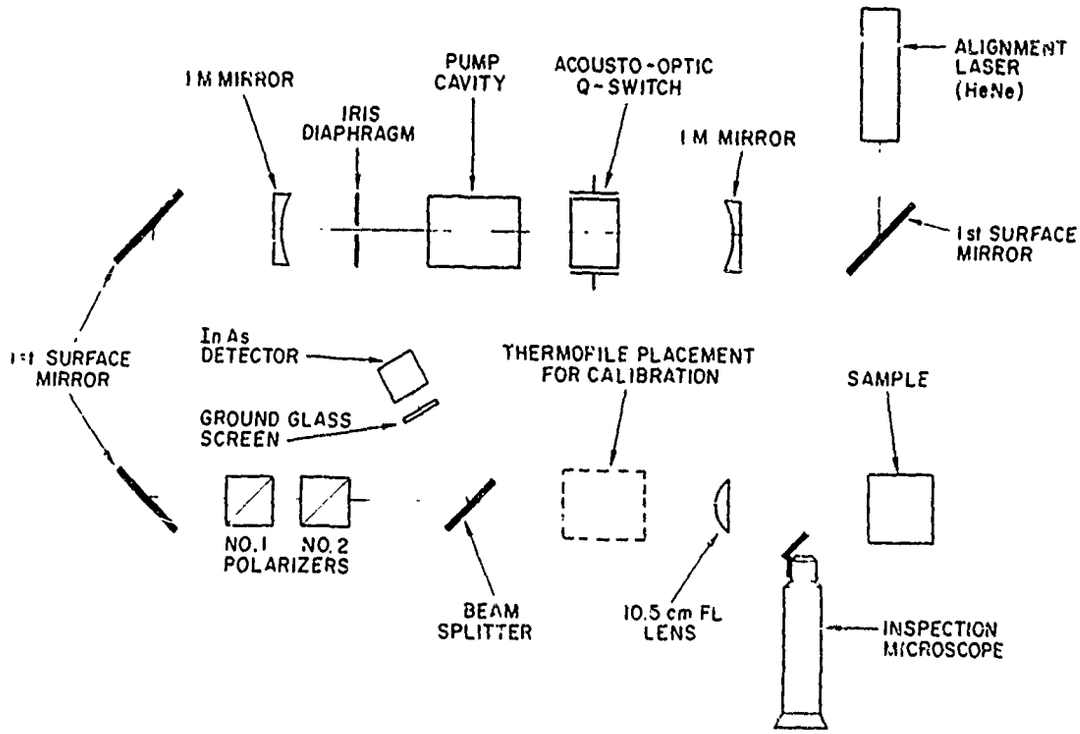

6. Experimental setup for proustite damage experiments using low power Nd:YAG laser.

The quality of the surface finish is important, not only for determining how easily the damage can be seen, but also in determining the type of damage that is visible as well as the threshold at which it occurs. Because proustite is so soft, it is virtually impossible to obtain by abrasive polishing an optical finish that is free of scratches. In addition, a freshly polished surface upon standing in air for a few hours begins to take on a cloudy appearance. This cloudiness increases slowly, and after a few days damage thresholds are appreciably lower than for the freshly polished surface. This fact was discovered in the latter stages of the study.

Therefore, in order to obtain meaningful and reproducible data for the detailed experiments in which the effects of pulse repetition rate were studied, the surface was periodically touched up whenever the thresholds began to drift downward. In the latter stages of this work, a cleaning procedure after polishing was employed, i.e., the surface was flushed with 1,1,2 trichloroethane, followed by alcohol and finally deionized water, and then dried with a fine jet of Freon from a pressurized container. This procedure effected results that were appreciably more reproducible than those obtained during the earlier stages of the program.

4. Damage in Proustite at 6328 Å

During the course of our damage experiments, we discovered another source of lack of reproducibility in damage thresholds with proustite. A He-Ne alignment laser was used to aid in locating the position of the Nd:YAG laser beam at various points in the experimental setup, including the surface of the sample. The intensity of the alignment laser beam and the time of exposure on the sample surface varied considerably, depending on the particular procedure taking place in the laboratory. It was found fairly late in the program that, in fact, appreciable damage can be created by the focused He-Ne laser beam. As usual, it is not a trivial matter to detect this damage visually and most of the time when it was seen, it was attributed to

the 1.06 μm radiation. The relative polarization of the light from the two lasers was such that as the light from the Nd:YAG laser was attenuated (by rotating the first of a pair of polarizing prisms), the light from the He-Ne laser incident on the sample was increased, leading to more confusion as to an interpretation of what was happening. No attempt was made to measure the intensity at which damage occurs at 6328 Å but an approximate upper limit is 4 W/cm^2. Needless to say, from that point on the He-Ne laser was not used to locate the beam position on the sample.

5. Damage Threshold in Proustite as a Function of Pulse Repetition Rate

After the reproducibility problem discussed earlier had been minimized, a series of threshold measurements were carried out on proustite at different pulse repetition rates. All the measurements were taken on the same sample. The results of these measurements are presented in Table II. The damage threshold intensities listed are those levels for which damage was observed according to the procedure described earlier in Section II-B-3.

It should be pointed out here that most of the sites where damage was observed at a particular power level were subjected to a large number of shots at predamage powers, which were a few percent below the level at which damage was finally seen to occur. A typical example is a damage site which at 60 pps was subjected to over 4,000 shots whose powers ranged in steps from 78 to 93% of the power at which damage finally occurred. We cite another example at 500 pps in which the site of interest was subjected to 30,000 nondamaging shots, whose powers ranged from 55 to 90% of the power at which damage occurred. Hence we interpret the range of threshold data obtained for proustite as reflecting a variation in surface damage resistance from point to point, rather than as reflecting an intrinsic probability for damage as inferred by Bass and Barrett in their studies of surface damage in a number of other materials.[3]

TABLE II

Damage Thresholds for Proustite

Wavelength, μm	Pulse Repetition Rate	Damage Threshold[a] Power Density, MW/cm^2		Damage Threshold Energy Density, J/cm^2	No. of Thresholds Measured
		Av Value	Range		
1.06	Single Shot	1.57	1.24 to 1.89	0.393	11
1.06	60 pps	1.61	1.40 to 1.89	0.403	11
1.06	300 pps	1.48	1.24 to 1.69	0.370	16
1.06	500 pps	1.50	1.24 to 1.73	0.376	10
0.694	Single Shot	60	54 to 69	1.08	10

[a]These values are given as total power (or energy) divided by the beam area defined as πa^2, where a is the 1/e radius for the electric field. The on-axis intensities (energy densities) are twice as large as the values quoted in the table.

T605

The damage threshold at 0.694 μm listed in Table II was measured early in the program on a different sample than the one for which the 1.06 μm data apply. The energy densities are in much closer agreement than the power densities and are probably the more meaningful quantities for comparison. Recently reported thresholds for proustite at 1.06 μm[4] fall in the range 12 to 45 MW/cm^2, yielding for the pulse widths used (17.5 nsec) energy densities of 0.21 to 0.79 J/cm^2. These values compare favorably with the values obtained at the same wavelength.

6. Damage in Proustite for Continuous Illumination at 1.06 μm

As mentioned in Section II-B-1, two kinds of damage occur with cw illumination: the molten craters and the speckled ghost sites. The first type occurs at relatively high cw powers and requires long exposure times (sometimes several minutes) before suddenly occurring. The conditions under which it occurs (power and exposure time) vary so drastically that we were unable to obtain meaningful quantitative data. A threshold for the latter type of damage also was difficult to define, but it is possible to quote some limiting conditions under which it occurs. The power density for which this speckling persists after five minutes was taken as one limit. This value is approximately 2.3 kW/cm^2. The power density at which no speckling was observable at all for several minutes of exposure is about 300 W/cm^2. Between these two values, the speckled ghost sites appear to varying degrees; after the laser is turned off, they fade and gradually disappear.

7. Ion Beam Sputtering of Proustite

Recently on another program, we observed a substantial increase in surface damage thresholds for sapphire crystals that were polished with energetic Ar^+ ion beams [5]. This preliminary success led us to attempt a few similar treatments with proustite. The results of early attempts to ion polish proustite caused severe deterioration of the sample at the surface being irradiated. The degradation led to a change in the sample color (from a red to a velvety grey-black) and also to a crumbling of the material at the edges and all along the surface. The first treatment was carried out at fairly high Ar^+ energy and current (7 kV at 300 $\mu A/cm^2$ for 4 hr). Subsequent ion polishing attempts under less severe conditions (2 kV for 45 min) showed no improvement in surface damage threshold. Under the above conditions, there was also no noticable improvement in the surface finish as far as scratch removal is concerned and possibly some indication of a slight deterioration similar to that seen for the high energy long exposure conditions first tried was present.

The nature of the proustite degradation with ion beam exposure is not known, but obvious chemical changes take place. It is possible that the origin is strictly thermal, and that some success can be realized for obtaining scratch-free surfaces using smaller ion energies and ion currents. These avenues should be pursued before reaching any definite conclusions as to the usefulness of ion beam polishing as a technique for improving proustite surfaces and damage thresholds.

8. Proustite Damage Thresholds in Vacuum

It was of some interest early in the program to resolve the question as to whether the proustite damage mechanism involves any interaction with oxygen in the atmosphere. A few experiments were carried out at 6943 Å using the single pulse ruby laser on the same sample, both in air and at about 1 Torr pressure. No change in damage threshold was obtained under the different conditions, leading to the conclusion, on the basis of these preliminary results, that the damage mechanism is not strongly influenced by the presence of air.

9. Proustite Protective Coating Experiment

A single attempt was made late in the program to apply a protective low reflectivity coating to proustite in anticipation of improving its damage threshold. What was intended to be a quarter-wavelength thick layer of sapphire was sputtered onto a proustite surface and damage thresholds measured. A substantial increase in surface damage threshold (up to 2 times) was observed for some regions of the coated crystal. Other regions had damage thresholds which were almost as low as that for the uncoated sample. A rough attempt was made to measure the transmission of the coated sample compared with the uncoated sample in order to infer the decrease in reflectivity but the results were difficult to interpret because of scatter in the data. This preliminary result is promising and suggests that the coating of easily

damaged materials such as proustite with more durable materials may be feasible to provide improved resistance. This phenomenon will be pursued in future work.

C. LASERS USED IN DAMAGE STUDIES

1. High Power Nd:YAG Laser

The high power Nd:YAG laser (as schematically illustrated in Fig. 1) is pulse excited by a Kr-arc pump lamp and electro-optically Q-switched. It has the capability of being triggered externally from single shot operation to maximum repetition rate of 10 pps or internally triggered at 10 pps. The Nd:YAG rod is 0.25 in. diameter by 2 in. long, pumped by the 2 in. arc length Kr lamp in a close coupling configuration. The output coupler is a flat 47% transmission mirror, and the high reflector (HR) used is a 53 cm radius-of-curvature mirror. To achieve single transverse mode control, the resonator cavity is internally apertured by a 2 mm diameter pinhole placed 14 cm from the HR mirror. The laser resonator is 52 cm in length.

At full output (i.e., no transverse mode control), the output energy is approximately 100 mJ/pulse with about a 20 nsec pulse width. However, when apertured to produce the desirable transverse mode profile, the output energy is reduced to about 7 mJ/pulse with an 18.5 nsec pulse width. For single shot operation, there exists a ±3% amplitude fluctuation in the pulse height from shot to shot. When operated at 10 pps, the amplitude fluctuation disappears and the output level is very stable. An oscilloscope trace of a typical output pulse for this laser is shown in Fig. 7.

2. Low Power Nd:YAG Laser

The low power Nd:YAG laser (as schematically shown in Fig. 6) is continuously pumped by a Kr-arc lamp and acousto-optically Q-switched. It has the capability of being operated continuously, singl

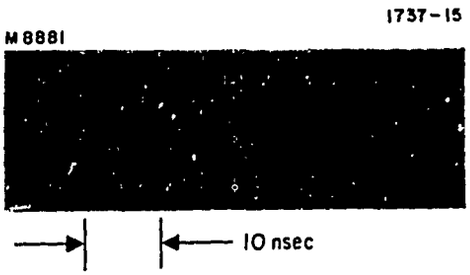

Fig. 7. Oscilloscope trace showing output of high power Nd:YAG laser.

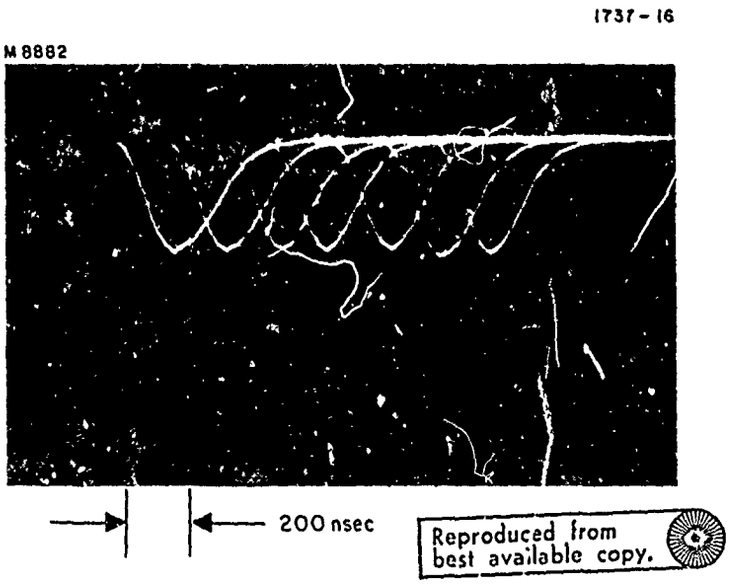

Fig. 8. Oscilloscope trace showing output of low power Nd:YAG laser for a number of consecutive shots.

pulsed, or repetitively Q-switched at rates up to 50 kHz. The pump cavity utilizes an elliptical cylinder 2 in. in length and having walls coated with evaporated gold. The Nd:YAG rod is 0.25 in. diameter by 2 in. long, while the Kr-arc lamp discharge is 2 in. long with a bore diameter of 4 mm.

The resonator cavity is formed by two 1 m radius-of-curvature mirrors separated by a distance of 65 cm. For the experiments, a 4.2% transmission output mirror was used. An internal aperture of variable diameter provided the transverse mode control. By decreasing the aperture size, the TEM_{00} output mode of the laser can be obtained by progressively eliminating the higher order transverse modes. The TEM_{00} is then selected with the collapse of the degenerate TEM_{10} mode. A UV excited IR phosphor screen is utilized for visual selection of the TEM_{00} mode.

At full power, multimode output of 54 W is obtainable using a single 2.5 kW Kr-arc lamp. However, due to the well-known thermally induced birefringence of the Nd:YAG rod, the TEM_{00} output was drastically reduced to approximately 1.5 W maximum. (No attempt was made to compensate the induced birefringence.) This resulted in peak powers of about 1 kW at low repetition rates (<500 pps). The peak power decreased monotically for high repetition rates. Pulse widths of between 180 to 250 nsec resulted, depending on the repetition rate used. Amplitude stability was ~ ±3% when the laser was properly adjusted. An oscilloscope photograph of a number of single shots showing the typical reproducibility for this laser is shown in Fig. 8.

3. High Power Q-Switched Ruby Laser

The experimental setup is shown in Fig. 9. The oscillator employs a 4 in. long by 0.25 in. diameter ruby, pumped by two linear lamps in a double elliptical pump cavity. The ruby crystal is water cooled by a closed cycle refrigeration system maintained at $0^{\circ}C$. The high reflectivity mirror is coated with a 99+% reflectivity high field damage coating from Perkin Elmer Corporation. Q-switching is

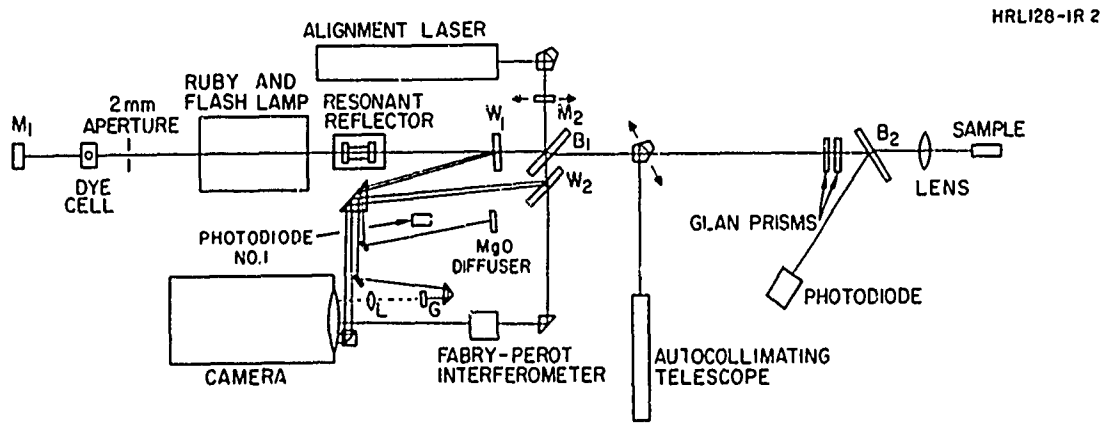

Fig. 9. Experimental setup showing pulsed ruby laser.

accomplished with a solution of cryptocyanine in methanol in a 1 mm path length cell whose transmission is 30% at 6943 A.

The temperature controlled (34°C) resonant reflector that was designed to optimize longitudinal mode control consists of two quartz etalons and a quartz spacer, whose combined effect is to enhance cavity modes separated by 2 cm^{-1} and to discriminate against intermediate modes.

Portions of the laser beam are split off in various ways (see Fig. 9), so that the power output, near and far field patterns, and Fabry-Perot patterns can be monitored for each shot. An oscilloscope trace of a typical output pulse for this laser is shown in Fig. 10.

4. CW and Repetitively Q-Switched Ruby Laser

The continuously pumped, repetitively Q-switched ruby laser can be operated either continuously or in a repetitively Q-switched mode (up to 2 kHz). The pump cavity is an elliptical cylinder 2 in. long, enclosing a ruby rod and a high pressure Hg-arc lamp. The ruby rod is 2 mm diameter by 2 in. long, while the Hg-arc lamp contains a 1 mm diameter bore and 2 in. discharge. The entire pump cavity is flooded with cooling water when the laser is in operation. The resonator cavity is formed by two 25 cm radius-of-curvature mirrors separated by a distance of 55 cm. Q-switching can be accomplished either with a rotating mirror Q-switch or an acousto-optic Q-switch. The former has a maximum repetition rate of ~400 pps, while the latter can Q-switch up to 2000 pps. The Q-switched output beam is predominantly TEM_{00}, because of the laser design. Typically, 20 kW peak powers can be obtained for repetition rates up to 400 pps. However, due to the high probability of surface damage to the ruby rod if foreign particles are present, the peak powers are limited to below 10 kW when in operation. Typical pulse widths range from 30 to 65 nsec for the range of repetition rates.

Due to the extreme demands on the high pressure Hg-arc lamp (>200 atmosphere pressure at 1000°C in the 1 mm diameter by 2 in. long

HRL 265-5

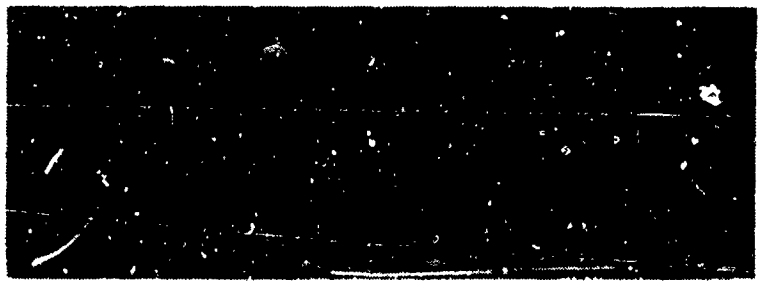

Fig. 10. Oscilloscope trace showing output of pulsed ruby laser with 20 nsec/division sweep rate.

volume of the discharge), the operating time of the laser is not predictable. Lifetime of the Hg-arc lamps range from a few minutes to 25 hours. Reliable operation of the laser can be achieved when lamp lifetimes can be made more predictable.

Table III compares the characteristics of the four laser types utilized for this program.

TABLE III

Characteristics of Lasers Used on Program

Properties	High Power Nd:YAG	Low Power Nd·YAG	High Power Ruby Laser	Low Power Ruby Laser
Wavelength	1.06 μm	1.06 μm	0.694 μm	0.694 μm
Operating Characteristics	Single shot to 10 pps	Single shot to 50,000 pps or cw	Single shot	Up to 2000 pps or cw
Mode Properties	TEM_{00}	TEM_{00}	TEM_{00}	TEM_{00}
Peak Power (Pulsed Mode)	300 kW	1 kW	~1MW	20 kW
Energy per Pulse	~6 mJ	~0.25 mJ	~15 mJ	1 mJ
Pulse Width (FWHM)	18.5 nsec	240 nsec	~20 nsec	~30 nsec
Av Single Mode CW Power	- -	1.5 W	- -	250 mW
Measured Beam Radius[a] at Lens Focus for Damage Experiments	25 μm	74 μm	56 μm	- -
Focal Length of Lenses Used in Damage Experiments	3.5 cm	11 cm	19 cm	19 cm

[a] The beam radius is defined here as the 1/e radius for the electric field.

T606

D. BEAM DIAGNOSTICS AND POWER CALIBRATIONS

1. Beam Diagnostics at 1.06 μm

Details of the beam spot sizes were determined by measuring the diameter of burn spots on unexposed developed Polaroid film for known incident powers ranging from the burn threshold to the maximum

power available from the laser. The measurements were made for the two Nd:YAG lasers employed in this program. For the low power Nd:YAG laser, spot size was determined at the position of the entrance surface of the proustite samples that were studied. This position is slightly upstream from the waist of the beam as it is focused by the 11 cm lens. The spot size for the high power Nd:YAG laser was measured at the waist beyond the 3.5 cm lens used for focusing the output inside the $LiIO_3$ samples that were studied.

For each laser, about 40 shots were taken for which burn spots were measured. The diameters of the burn spots were measured using an optical microscope with a calibrated reticle at 200X magnification. The technique was found to be surprisingly well suited to this sort of measurement. It was found that the burn spots are extremely well defined, in that the boundary between the burned and unburned regions of the film is very sharp. Examples of burn spots are shown in Fig. 11. The validity of this technique is based on the assumption that the film possesses a sharp burn threshold and that the diameter of a given burn spot is equal to the beam diameter at which the intensity (or energy density) equals the burn threshold.

The following expression would then apply for gaussian beam:

$$I_t = I_o \exp(-d_t^2/4a^2) \qquad (1)$$

where I_o is the peak intensity, I_t is the intensity at burn threshold, d_t is the diameter of the burn spot, and a is the characteristic 1/e radius for the intensity.

Taking logarithms we have:

$$\ell n\, I_o = d^2/4a^2 + \ell n\, I_t \qquad (2)$$

From eq. (2) we see that a semilog plot of peak power versus the square of the burn spot diameter should give a straight line with slope equal to $1/4a^2$ and intercept equal to $\ell n\, I_t$ for a gaussian beam

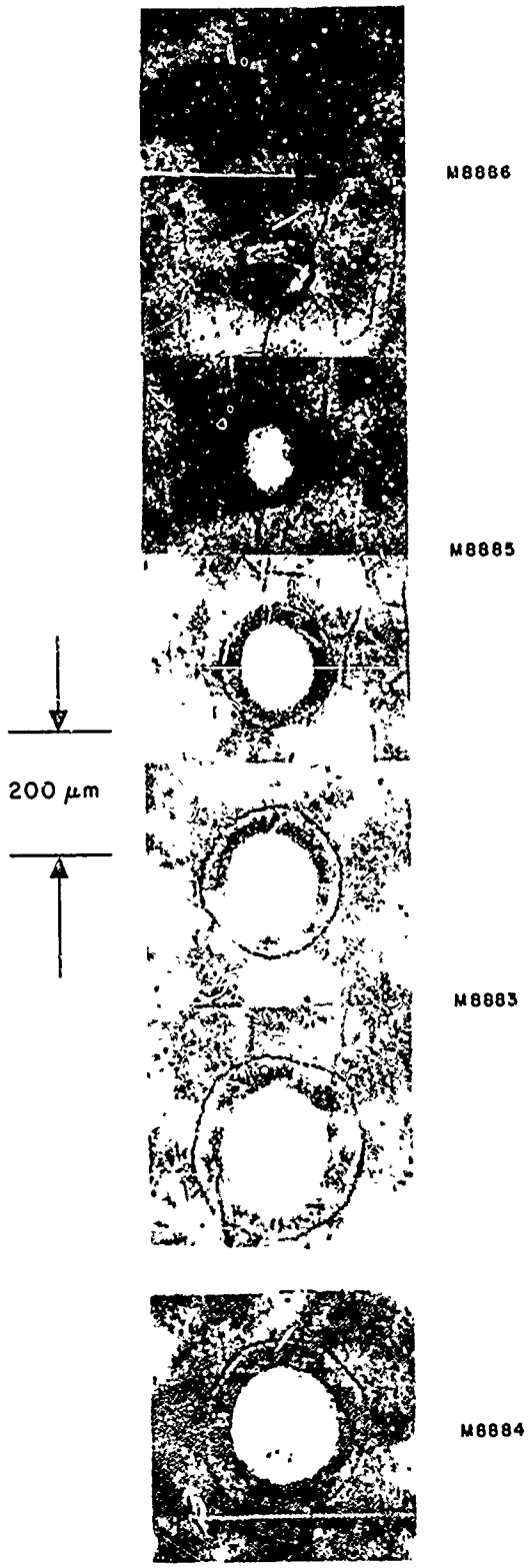

Fig. 11. Photomicrographs of Nd:YAG laser burn spots for different incident powers.

profile. Deviations from gaussian behavior will be evidenced as curvature in these plots. Data for the two Nd:YAG lasers are plotted in Figs. 12 and 13. Deviations from linearity are evident at the high power end of these plots (corresponding to the wings of the distribution), and the curvature is such that the actual beam profile contains more energy in the wings than an ideal gaussian distribution. That is, the burn spots formed at high powers are larger than those expected for gaussian beams.

From the slopes in Figs. 12 and 13, we obtain values for a, the 1/e radius for the intensity of 18.0 ± 1.5 μm for the high power laser (Fig. 12) and 52.5 ± 3 μm for the low power laser (Fig. 13). The corresponding values for $\alpha = \sqrt{2}a$, the 1/e radius for the field (also the $1/e^2$ radius for the intensity) are 25 and 74 μm, respectively.

2. Beam Diagnostics at 6943 Å

A detailed series of beam profile and spot size measurements on the single pulse ruby laser have been carried out in connection with another program[6]. The beam was photographed using a multiple exposure camera incorporating nine lenses, each one having a different amount of optical attenuation. Hence, each photograph contains nine different exposures of the same spot. By taking densitometer scans of the different spots, detailed information can be obtained about the spatial beam profile without requiring knowledge of the film response characteristics[7]. The results of a series of beam profile measurements are included in Reference 6. The far field spatial profile was found to be gaussian down to 8% of the peak. The spot size at the beam waist under the focusing conditions (19 cm lens) for the experiments carried out in this program for the pulsed ruby laser is 56 μm radius at the 1/e points for the electric field.

3. Power Calibration Measurements

For the pulsed ruby and high power pulsed Nd:YAG lasers, the output energy was measured using a calibrated Hadron thermopile and

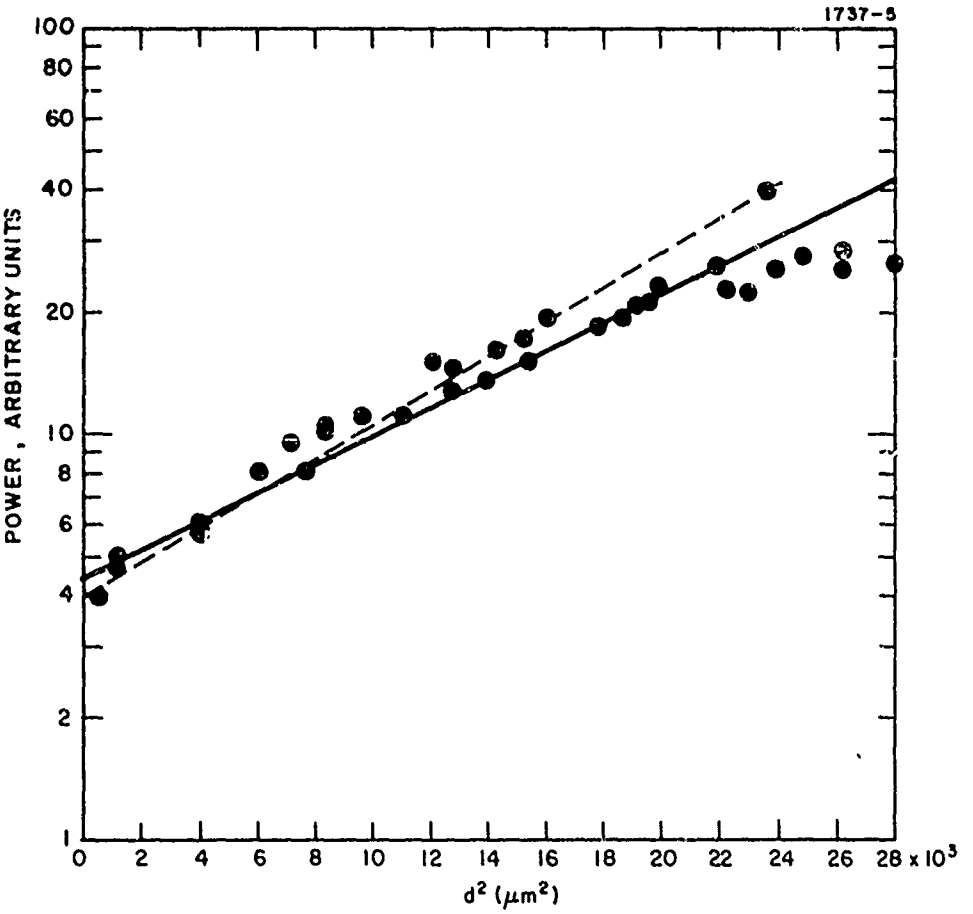

Fig. 12. Log P versus d^2 for burn spots taken at focus for low power Nd:YAG laser.

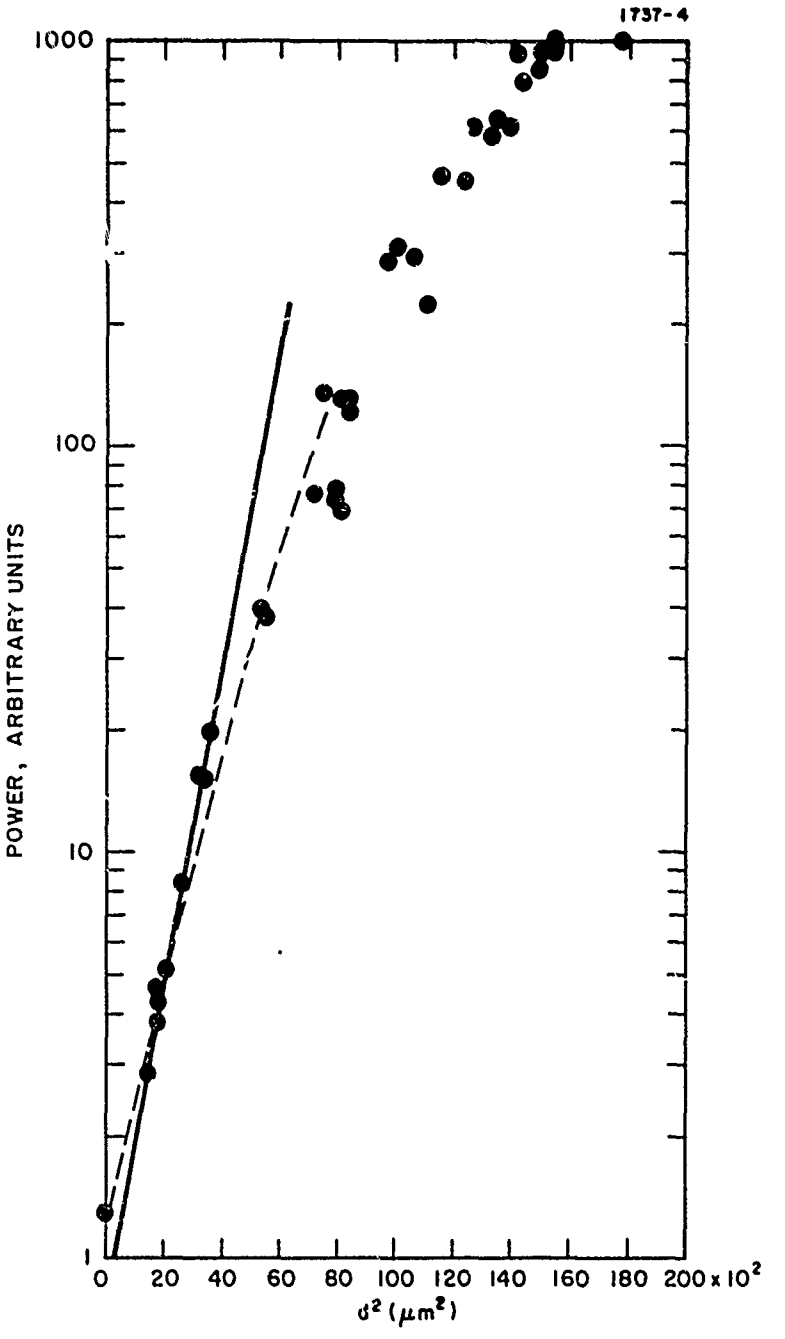

Fig. 13. Log P versus d^2 for burn spots taken at focus for high power Nd:YAG laser.

by simultaneously comparing the measured energy with the output of the monitoring Si photodetectors. From that point, the Si photodiodes were used as secondary standards. The energy of a single pulse was measured with the ruby laser while the total energy in a series of ten pulses was typically measured for the Nd:YAG laser operating at 10 pps. The energy per pulse was then obtained by dividing the total energy by the number of pulses. Temporal peak powers quoted in this report are obtained by dividing the total energy per pulse by the pulse width (FWHM). Power calibrations for the low power Nd:YAG laser were carried out by measuring the average power in the beam using a CRL Model 201 power meter while the laser was operating at a given known pulse repetition rate and simultaneously monitoring the output of the InAs photodetector. Hence, from a knowledge of the repetition rate, average power, and pulse width, values of peak power and energy per pulse can be obtained.

SECTION III

CONCLUSIONS

The program studies reported here, within the bounds of the specified objectives, revealed several significant findings. In spite of the fact that there remain questions yet unanswered, our findings have elicited much valuable information.

This section concludes with a summation comparision of the two subject materials.

A. $LiIO_3$ DAMAGE RESULTS

We conclude that the threshold for laser induced bulk damage in $LiIO_3$ is independent of whether the crystal is phase matched for second-harmonic generation under the conditions of our experiments. The experimental conditions upon which this conclusion is based are:

- Single pulse operation at 0.694 μm and 1.06 μm
- 10 pps operation at 1.06 μm, with ~20% second-harmonic conversion for both conditions.

Without further research, proof that this conclusion would be valid or different under high average power conditions such as exist in cw intracavity systems cannot be offered.

B. PROUSTITE DAMAGE RESULTS

The fact that the damage threshold for proustite surface damage is independent of pulse repetition rate over the range studied suggests that the mechanism is not an average power phenomenon, at least for the one type of damage studied most extensively. Proustite behavior is complicated by the fact that different types of damage can occur, and that at low levels of cw illumination the damage is noncatastrophic, i.e., the crystal appears to heal itself. A comparison of our results with those of Hatna et al.,[4] who measured thresholds for pulses

considerably shorter than those measured at HRL (18 nsec versus 240 nsec), indicates that pulse energy density is the more meaningful quantity to define threshold rather than peak power density. (Unfortunately, within the scope of this program we were not in a position to explore the damage threshold for proustite at shorter pulse lengths for verification of their results.) Also, our results with the pulsed ruby laser show better agreement when the energy densities rather than power densities are compared for the two wavelengths, although there is no a priori reason that the thresholds should be expected to be the same at the two wavelengths. Nevertheless, these results indicate that over the range of conditions studied, damage occurs when a minimum energy is deposited per unit area. This suggests that the mechanism involves an absorption of energy at or near the surface in a sufficiently short time that decomposition can occur before the energy can be dissipated. In addition, there appears to be another mechanism that is average-power dependent, but the damage that occurs under these conditions is very difficult to define because of its transitory nature.

REFERENCES

1. R. Webb, Damage in Laser Materials: 1971, edited by A. J. Glass and A. H. Guenther, NBS Special Publication 356, 1971 (U.S. GPO, Washington, D.C.) p. 98. For a general set of references on laser induced damage, see also NBS Special Publication 341 (1970).

2. G. Nath, communicated at the Sixth International Quantum Electronics Conference, Kyoto, Japan, 1970.

3. M. Bass and H. Barrett, IEEE-JQE 8, 338 (1972).

4. D. C. Hanna, B. Luther-Davies, H. N. Rutt, R. C. Smith, and C. R. Stanley, IEEE-JQE 8, 317 (1972).

5. C. R. Giuliano, Appl. Phys. Letters 21, 39 (1972).

6. C. R. Giuliano, D. F. DuBois, R. W. Hellwarth, and G. R. Rickel, Damage Threshold Studies in Laser Crystals, HRL Semiannual Report 3 (Jan. 1971) AFCRL-71-0064.

7. I. M. Winer, Appl. Optics 5, 1437 (1966).